Vietnam Journal of Science and Technology ***58*** *(5A) (2020) 170-179*

doi:10.15625/2525-2518/58/5a/15289

ACTIVATED CARBON FABRICATED FROM VIETNAMESE SUGARCANE BAGASSE FOR REMOVAL OF CIPROFLOXACIN FROM AQUEOUS SOLUTION: PREPARATION, CHARACTERIZATION AND KINETIC STUDIES

Lam Van Tan[1, 2], To-Uyen T. Dao[2, 3], Hong Tham T. Nguyen[2, 3], Trinh Duy Nguyen[2, 3], Long Giang Bach[2, 3, *]

[1]*Center of Excellence for Functional Polymers and Nano Engineering, Nguyen Tat Thanh University, Ho Chi Minh City, Viet Nam*

[2]*NTT Hi-Tech Institute, Nguyen Tat Thanh University, Ho Chi Minh City, Viet Nam*

[3]*Center of Excellence for Green Energy and Environmental Nanomaterials (CE@GrEEN), Nguyen Tat Thanh University, 300A Nguyen Tat Thanh, District 4, Ho Chi Minh City, Viet Nam*

[*]Email: *blgiang@ntt.edu.vn*

Received: 15 July 2020; Accepted for publication: 24 August 2020

Abstract. Recent interest in wastewater treatment has shifted to the use of agricultural waste to treat antibiotics in aqueous solutions due to the economic efficiency the technique brings. This study focuses on the synthesis, properties and study of the kinetic mechanism of activated carbon and its potential application to remove antibiotics from aqueous solutions. Activated carbon is synthesized from sugarcane bagasse by activated method with active substance of $ZnCl_2$. With a specific surface area of about 980.84 m^2/g and high porosity, the product could absorb a large amount of ciprofloxacin (CIP) antibiotics. The properties of materials are characterized by relevant analytical techniques such as scanning electron microscopy (SEM), X-ray diffraction (XRD), Fourier transform infrared spectroscopy (FTIR) and Brunauer-Emmett-Teller (BET). The behavior of CIP adsorption was studied under the effect of adsorption dose, initial CIP concentration and pH value. The adsorption and isothermal mechanisms are also studied. The results show that the adsorption adhered to the second kinetic model and the experimental data was found to be reasonably fitted to the Langmuir isotherm. Therefore, activated carbon manufactured from sugarcane bagasse could be used as a potential adsorbent to effectively remove antibiotics from aqueous solution.

Keywords: ciprofloxacin, activated carbon, adsorption, isotherms, kinetic studies.

Classification numbers: 3.4.2, 3.6.1, 3.7.4.

1. INTRODUCTION

The prevalence of antibiotic residues in water environment has become an emerging threat to humans and the ecosystem. Among antibiotics, ciprofloxacin (CIP), a synthetic antibiotic of the quinolone group, has been found in high concentration (about 31 mg/L) in effluent from drug industries and even in common wastewater. The antibiotic is a widely used substance to treat bacterial and human infections in humans [1 - 3] and could be released directly into natural

waters in large quantities due to the incomplete metabolism of humans and animals [4]. In addition, inexhaustive eradication of CIP residues in sewage and surface water may result in the promotion of antibiotic-resistant bacteria, leading to further harm to human health and the ecosystem.

Given the limitations of conventional methods such as biodegradation, photovoltaic, oxidation and the increasing threat of antibiotics contamination, efficient, sustainable and economical technologies are therefore essential. Adsorption is a technique that requires simple implementation, has low cost and high efficiency and generates considerably less toxic intermediates. To achieve high adsorption separation efficiency, it is necessary to develop adsorption materials with fast adsorption speed, high selectivity and good adsorption capacity. In recent years, porous carbon like activated carbon (AC) has received a great deal of attention because of its high specific surface area, the large pore volume of functional groups on the material surface and low cost. However, one main drawback of AC is the expensive precursor that is required for AC synthesis, thus limiting the application of the adsorbent. Recent advances in materials science have suggested agricultural waste as a renewable, cheap and widely available source for the synthesis of AC. Successful utilization of such sources could significantly contribute to the reduction of environmental abatement cost, improve the quality of life in rural and remote areas and open up new pathways for discovery of more efficient materials used for water decontamination. Therefore, in this study, we have studied the use of bagasse as a precursor to synthesize activated carbon for CIP treatment in water. Bagasse after carbonization is activated chemically, followed by potassium hydroxide (KOH) and heated at a temperature of 500 °C in a nitrogen furnace. The as-synthesized AC was characterized by modern analysis techniques, such as X-ray diffraction (XRD) method, Scanning electron microscopy (SEM), Fourier transform infrared spectra (FTIR) and Brunauer-Emmett-Teller (BET), and subjected to further adsorption evaluation for determination of adsorption capacity and suitable kinetic model.

2. MATERIALS AND METHODS

2.1. Synthesis of activated carbon from sugarcane bagasse

Bagasse was dried in the sun for 2 - 3 days, then crushed and sifted with a mesh of 210 mesh/cm^2. Following that, 20 g of dry sugarcane bagasse powder was activated with $ZnCl_2$ at 1:1 ratio (g/g) in 24 hours. To form AC, the impregnated sample was then dried for 24 hours at 105 ^oC with 99.9 % N_2 gas flow at 500 ^oC layers to peel off and afford the physical carbonization stage, eventually leading to expansion of the volume of the material. After that, activated carbon was soaked with distilled water several times and then washed with 2 % HCl until pH reached 7. Finally, dry activated carbon was finely ground and stored for further use.

2.2. Characterization of activated carbon

The crystal structure of the material was confirmed by XRD (on the D8 Advance Bruker), using Cu Kα stimulation with a scanning rate of 0.030º/s in the 2θ region from 5 - 80º. The crystal morphology of the material was observed through a scanning electron microscope (JSM 7401F, Jeol). The light absorption properties of the material were analyzed via Diffuse Reflectance Spectroscopy (UV-Vis-DRS, Shimazu UV-2450) in the 300-900 cm range of waves -first.

2.3. Batch adsorption studies

The effect of initial concentration, pH and reaction time on CIP adsorption capacity was carried out in a batch in 250 mL conical flasks at 29 °C. Adsorption experiments were performed by adding 1 g/L adsorbent (AC) to 100 mL CIP solution (20 - 80 mg/L). The pH was adjusted in the range of 2 - 12 with HCl and NaOH solutions. The adsorption occurred in a shaking environment with a speed of 200 rpm in the specified time period. Next, the samples were centrifuged to separate the solution from the adsorbent. Finally, the concentration of the remaining antibiotic was determined by the intensity change of absorption peak at 497 nm using a UV-visible spectrophotometer (Model Evolution 60S, Thermo Fisher Scientific). Adsorption capacity was calculated based on concentration before and after adsorption process according to the following equations:

$$H\ (\%) = \left(1 - \frac{C}{C_o}\right) * 100$$

where, C_o and C_e are, respectively, the initial and equilibrium antibiotic concentrations (mg/L).

3. RESULTS AND DISCUSSION

3.1. Structural characterization

The surface morphology of AC analyzed by SEM is shown in Figure 1. Visually, obtained activated carbon was highly porous with a honeycomb-like structure. The observed hard carbon skeleton with a rudimentary pore structure is the result of the pyrolysis process that took place to abolish non-carbon elements such as hydrogen, oxygen and nitrogen released on the AC surface. This in turn contributes to the increased surface area and improved adsorption of AC. The chemical bonds on the surface of the adsorbent were determined by the FTIR spectra in the range 4000 - 400 cm^{-1} and mentioned in Figure 2(a). A strong adsorption band observed in the region of 3076 - 3580 cm^{-1} is assigned to stretching vibration O-H derived from intermolecular hydrogen bonds linking with carboxylic acid. The adsorption peaks located around 2903 cm^{-1} and 2374 cm^{-1} show the stretching vibration of the C-H and C=C functional groups. Angular deformation in the bonding plane of C-H aromatic rings was indicated by adsorption peaks located in the range of 1000 - 1300 cm^{-1}. The presence of nitrogen compounds in the AC structure is confirmed by the extended peak of the N-H link in the 3689 - 4000 cm^{-1} range. Visually, the presence of functional groups such as hydroxyl and carboxyl groups on the surface of biological adsorbent is imperative for antibiotic adsorption [5]. The structure of AC is characterized by X-ray diffraction and the results were shown in Figure 2(b). XRD pattern of AC with typical characteristics has a strong diffraction peak at $2\theta = (23.7^o)$, which reveals the predominant amorphous structure [6, 7], which is a typical property of porous AC.

Nitrogen adsorption is an effective method to determine the properties of activated carbon, including porosity, surface area, pore volume, pore size. Inherent structure and the nitrogen adsorption/ desorption isotherm of ACs can be further elaborated and measured at 77 K, as illustrated in Figure 3. The hysteresis observed between desorption and adsorption featured in the obtained isotherm indicates the abundance of mesopores and micropores in the AC structure [8]. The surface area of the synthesized adsorbent, characterized by the BET technique, illustrate that AC manufactured from bagasse has high specific surface area. Further calculations following BET theory indicated that the surface area and pore volume of AC are 980.84 cm^2/g and 0.154 cm^3/g, respectively.

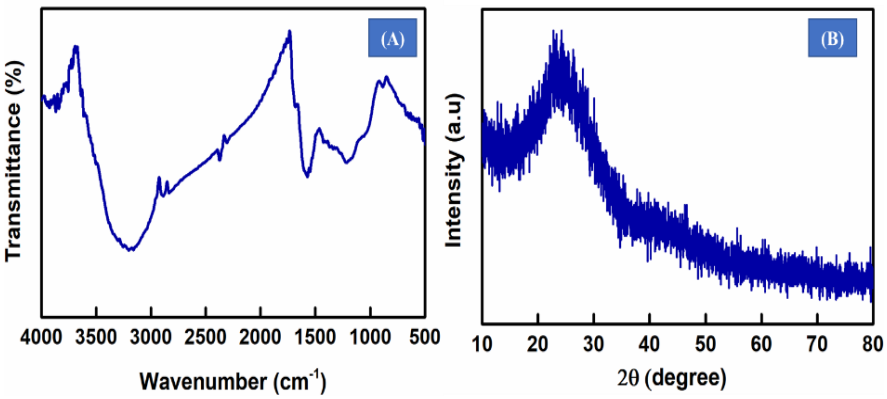

Figure 2. FT-IR spectra (A) and XRD images (B) of AC from sugarcane bagasse.

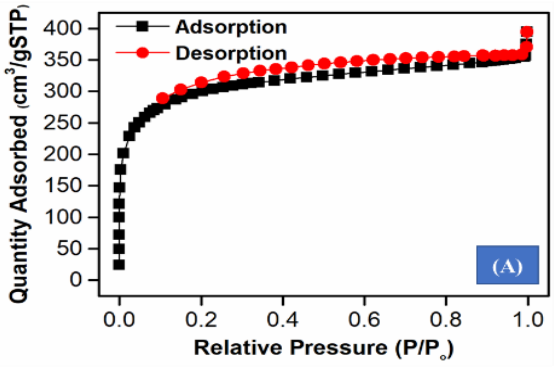

Figure 3. The N_2 adsorption/desorption isothermal of AC from sugarcane bagasse.

Table 1. The textural properties of AC from sugarcane bagasse.

Precursor	BET Surface Area (m^2/g)	Brunauer-Joyner-Halenda (BJH) Desorption Average Pore Diameter (4V/A) (nm)	BJH Desorption Cumulative Pore Volume (cm^3/g) (17–3000 A0)
Sugarcane bagasse	980.84	3.37	0.154

Table 2. Comparison of BET surface areas from different biomasses.

Biomass	S_{BET} (m^2/g)	References
Banana peel	63.5	[9]
Pineapple crown	39-700	[10]
Orange peels	300-620	[11]
Corncob	290.2	[12]
Sugarcane bagasse	829	[13]
Sugarcane bagasse	980.84	This study

Therefore, activated carbon from sugarcane bagasse is expected as a potential material to treat CIP in aqueous media. For comparison, Table 1 reported surface areas of adsorbents obtained from different biomasses.

3.2. Effect of AC dosage, contact time and initial CIP concentration on adsorption efficiency

CIP removal efficiency in relation to adsorbent dosage at a concentration of 40 ppm was described in Figure 4(a). As the adsorbent dosage increased from 0.5 to 1.5 g/L, the amount of CIP adsorbed onto AC increased from 59.6 % to 95.59 %. However, when the amount of adsorbent increased thereafter and approximated 3 g/L, the removal rate was only improved by 5 %.

The adsorption behavior of antibiotics on AC was examined with respect to different time periods ranging from 0 to 240 minutes and at three CIP concentrations. The results were shown in Figure 4(b) where rapid adsorption of CIP onto AC was observed within the first 60 min. Thereafter, with longer contacting time, the adsorption rose more steadily, and the equilibrium state was attained after 120 min. The maximum efficiency removal CIP is at 98 % and 86 % for 20 ppm and 40 ppm, respectively.

With regard to initial CIP concentration, when increasing the concentration to 80 ppm, the removal percentage plunged to about 65 %, which is supposed to be a result of insufficient binding sites on AC for a large number of antibiotic molecules. The CIP adsorption capacity is found in order: 19.64 mg/g (20 ppm) < 34.56 mg/g (40 ppm) < 52.98 mg/g (80 ppm).

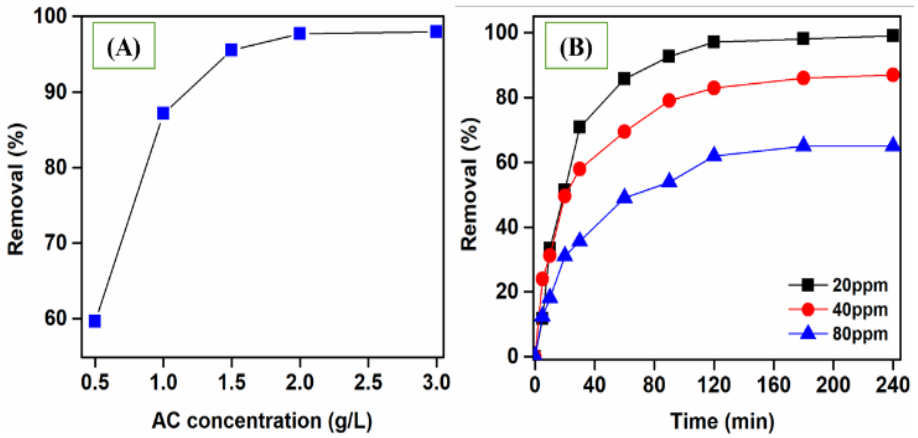

Figure 4. The effect of AC dosage (a), contact time and CIP concentration (b) on the adsorption capacity of AC for CIP.

3.3. Adsorption kinetics

Adsorption kinetic curves were estimated to predict adsorption rates, determine adsorption mechanisms and provide important information to design suitable adsorption systems [14]. The application of kinetic models allows clarification of the mechanism of antibiotic adsorption on AC. Kinetic adsorption data were studied by four common kinetic equations: first-order kinetics, second-order kinetics, Elovich and Bangham. Table 3 shows the kinetic parameters and results of adsorption process, Figure 5 shows the correlation of experimental adsorption data. With a low R^2 correlation coefficient (0.964 - 0.986), it is indicated that first-order kinetic lines did not

fit well with the experimental adsorption data. In contrast, high coefficient of determination R^2 (0.997 - 0.999) at all CIP concentrations and the consistency between $qe_{(theo)}$ value and the $qe_{(exp)}$ value shows the relevance of the quadratic model with most of adsorption data. Moreover, the adsorption data points were calculated to be more linearly distributed in the case of the quadratic model, as opposed to the result of the first order model. Therefore, the CIP adsorption process to AC is in accordance with the second-order kinetic equation, suggesting the mechanism of chemical adsorption through the interaction of adsorbents and functional groups on the surface of the material [15]. The Elovich equation, which describes a solid/gas adsorption through heterogeneous adsorption surfaces, and Bangham-like equation, which describes diffuse pore diffuse behavior were adopted to explain the adsorption process [16, 17]. As shown in Table 3, the kinetic data of the Elovich model show more relevance to experimental data than the Bangham model, indicating a heterogeneous diffusion on the surface. At the same time, the Bangham kinematic lines that do not pass through the origin point suggest that CIP penetration into the pores of AC is not the only step to control the adsorption rate. Other kinetic processes have occurred simultaneously and are capable of contributing to the adsorption mechanism [15, 18 - 20].

Table 3. Kinetic constants for the adsorption of CIP onto AC adsorbent.

Models	**Parameters**	**Concentrations (mg/L)**		
		20	**40**	**80**
Pseudo-first-order $\log(Q_1 - Q_t) = \log Q_1 - \frac{k_1.t}{2.303}$	k_1(min^{-1}/$(mg/L)^{1/n}$)	0.0269	0.0201	0.0213
	Q_1 (mg/g)	15.119	23.826	48.228
	R^2	0.9674	0.9798	0.9867
Pseudo-second-order $\frac{t}{Q_t} = \frac{1}{k_2.Q_2^2} + \frac{t}{Q_2}$	k_2 (g/(mg.min))	0.00252	0.00148	0.00062
	Q_2 (mg/g)	21.482	37.188	59.136
	$H = k_2Q_2^2$	1.1629	2.0467	21.7167
	R^2	0.9980	0.9993	0.9972
Elovich $Q_t = \frac{1}{\beta}.\ln(\alpha.\beta) + \frac{1}{\beta}.\ln(t)$	β (g/mg)	0.2300	0.1001	0.0857
	α (mg/(g.min))	2.5818	11.9214	25.4836
	R^2	0.9495	0.9791	0.9888
Bangham $\log\log\left(\frac{VC_o}{V.C_o - Q_t.m}\right) =$ $\log\left(\frac{k_B}{2.303.V}\right) + \alpha_B.\log(t)$	k_B (mL/(g/L))	$7.17*10^{-3}$	0.0121	$7.17*10^{-3}$
	α_B	0.7873	0.5413	0.5238
	R^2	0.9878	0.9762	0.9802

3.5. Effect of concentration and adsorption isotherms

The adsorption isotherm models are used to monitor the characteristics of the liquid and gas phase adsorption process when equilibrium is reached [3], which is insightful when it comes to designing an appropriate adsorption system. The different adsorption isotherms were studied for CIP adsorption on AC such as: isothermal lines Langmuir, Freundlich, Temkin and Dubinin – Radushkevich (D–R). Among them, Langmuir isotherm assumes homogeneous adsorbent surfaces and identical bonding positions on the material surface.

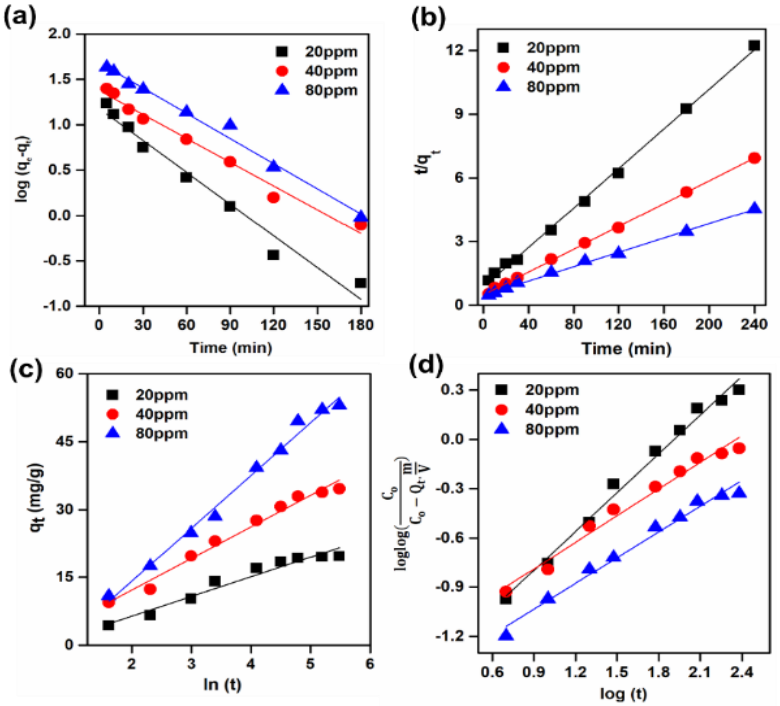

Figure 5. Kinetic plots of kinetic models: (a) pseudo first-order, (b) pseudo second-order, (c) Elovich and (d) Bangham for the adsorption of CIP onto AC.

Table 4. Isotherms constants for the adsorption of CIP onto AC adsorbent.

Models	**Parameters**	**Values**
Langmuir (8):	k_L (L/mg)	0.4167
$\frac{1}{Q_e}=\left(\frac{1}{Q_m K_L}\cdot\right)\frac{1}{C_e}+\frac{1}{Q_m}$	Q_m (mg/g)	57.142
	$R_L = 1/(1+K_L C_o)$	0.291
	R^2	0.9862
Freundlich (9):	k_F (mg/g)/(mg/L)$^{1/n}$	25.033
$\ln Q_e = \ln K_F + \frac{1}{n}\ln C_e$	1/n	0.1970
	R^2	0.8756
Temkin (10):	k_T (L/mg)	58.5705
$Q_e = B_T \ln K_T + B_T \ln C_e$	B_T	6.4301
	R^2	0.7535
D-R (11):	B (kJ^2/mol^2)	3.27*10^{-5}
$\ln Q_e = \ln Q_m - B\varepsilon^2$	Q_m (mg/g)	36.996
	E (kJ/mol)	123.65
	R^2	0.3566

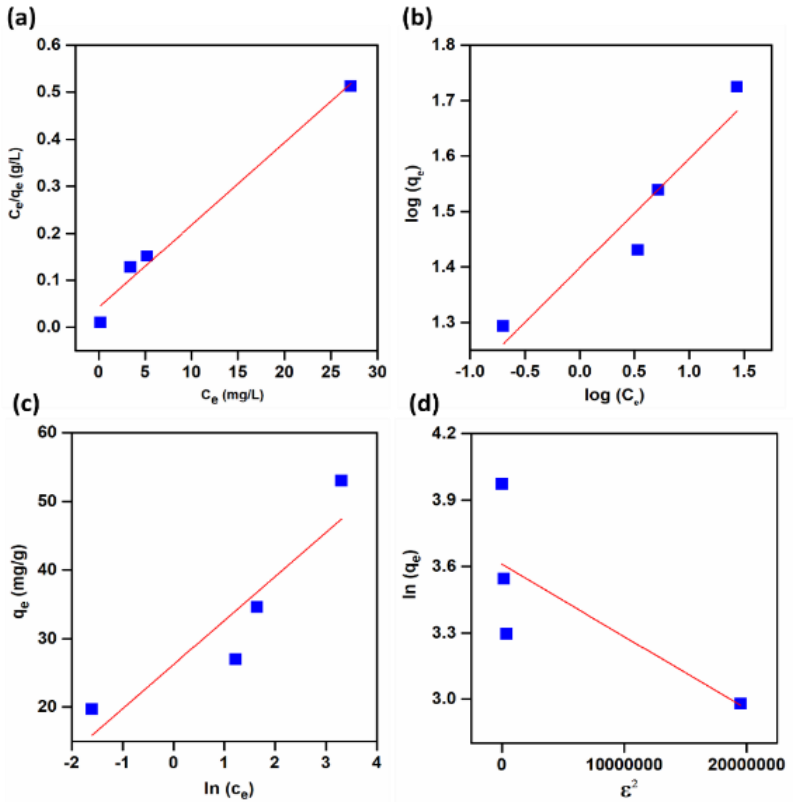

Figure 6. Linear plots of isotherm models: (a) Langmuir, (b) Freundlich, (c) Temkin, and (d) D-R for the adsorption of CIP onto AC.

The Freundlich isotherm assumes that the adsorbent surface is heterogeneous. Besides, the Temkin isothermal line implies that the adsorption is characterized by a uniform distribution of the binding energy and that the adsorption heat will decrease linearly with the coverage due to adsorption and contour lines. Thermal D-B is applied to test the properties, free energy and porosity of adsorbents [20, 21]. The isothermal equations and the results of the CIP isothermal process are summarized in Table 4.

With the R^2 coefficient of correlation ($R^2 > 0.98$) and the closeness of experimental data points to the linear line, as shown in Figure 6, it is suggested that CIP adsorption on AC follows the Langmuir model. Single-layer adsorption mechanisms are more likely to dominate other adsorption mechanisms. The maximum adsorption capacity attained 57.612 mg/g, calculated from the Langmuir isothermal equation. At the same time, the R^2 constant of the Langmuir model lies in the range of 0 - 1 and the coefficient of the Freundlich model as 1/n <1 shows the favorable adsorption of CIP to AC. In addition, the average free energy of adsorption Ea calculated from the D-B equation was greater than 8 kJ/mol, indicating that the adsorption on the Carbon atoms is chemical adsorption [21].

4. CONCLUSIONS

Charcoal char from the bagasse was successfully synthesized by activating $ZnCl_2$. The typical results show that AC shows a porous, amorphous carbon structure, having a relatively

high surface area of 980.84 cm^2/g. The adsorption results show that at equilibrium time of 120 minutes, the adsorbent dose of 1.5 g/L resulted in CIP removal efficiency of 95.59 %. Moreover, the kinematic and isothermal models indicated that CIP uptake to AC follows the chemical adsorption mechanism and monolayer adsorption behavior. The maximum adsorption capacity obtained from the Langmuir isotherm model for ACs was calculated as 57.142 mg/g, indicating that activated carbon from bagasse could be a potential adsorbent of CIP antibiotics in wastewater.

Acknowledgements. This research is funded by Vietnam National Foundation for Science and Technology Development (NAFOSTED) under grant number 104.05-2018.336.

REFERENCES

1. Fu H., Li X., Wang J., Lin P., Chen C., Zhang X. and Suffet I. H. (Mel) - Activated carbon adsorption of quinolone antibiotics in water: Performance, mechanism, and modeling, J. Environ. Sci. (China) **56** (2017) 145-152.
2. El-Shafey E. S. I., Al-Lawati H., Al-Sumri A. S. - Ciprofloxacin adsorption from aqueous solution onto chemically prepared carbon from date palm leaflets, J. Environ. Sci. (China) **24** (2012) 1579–1586.
3. Li R., Wang Z., Guo J., Li Y., Zhang H., Zhu J., Xie X. - Enhanced adsorption of ciprofloxacin by KOH modified biochar derived from potato stems and leaves, Water Sci. Technol. **77** (4) (2018) 1127-113.
4. Carabineiro S. A. C., Thavorn-Amornsri T., Pereira M. F. R., Figueiredo J. L. - Adsorption of ciprofloxacin on surface-modified carbon materials, Water Res. **45** (15) (2011) 4583-4591.
5. Sugumaran P., Susan V. P., Ravichandran P., Seshadri S. - Production and Characterization of Activated Carbon from Banana Empty Fruit Bunch and Delonix regia Fruit Pod, J. Sustain. Energy Environ. **3** (2012) 125-132.
6. Thuan T. V., Thinh,P. V., Thi B., Quynh P., Cong H. T., Thi D., Tam T. - Production of Activated Carbon from Sugarcane Bagasse by Chemical Activation with ZnCl2 : Preparation and Characterization Study, Res.J.chem.sci. **6** (5) (2016) 42-47.
7. Tran T. V., Thi Q. B., Nguyen P. D., Thi H. N. L., Bach L. G. - A comparative study on the removal efficiency of metal using sugarcane bagasse- derived ZnCl2 activated carbon by the response surface methodology, Adsorp. Sci. Technol. **35** (2016) 72-85.
8. Chaiwon T., Jannoey P., Channei D. - Preparation of Activated Carbon from Sugarcane Bagasse Waste for the Adsorption Equilibrium and Kinetics of Basic Dye, Key Eng. Mater. **751** (2017) 671-676.
9. Thuan T. V., Quynh B. T. P., Nguyen T. D., Ho V. T. T., Bach L. G. - Response surface methodology approach for optimization of Cu2+, Ni2+ and Pb2+ adsorption using KOH-activated carbon from banana peel, Surfaces and Interfaces **6** (2017) 209-217.
10. Taer E., Apriwandi A., Ningsih Y. S., Taslim R. - Preparation of Activated Carbon Electrode from Pineapple Crown Waste for Supercapacitor Application, Int. J. Electrochem. Sci. **14** (2019) 2462-2475.
11. Fernandez M. E., Ledesma B., Román S., Bonelli P. R., Cukierman A. L. - Development and characterization of activated hydrochars from orange peels as potential adsorbents for

emerging organic contaminants, Bioresour. Technol. **183** (2015) 221-228.

12. Kumar J., Kaur M., Adiraju B. - Synthesis of activated carbon from agricultural waste using a simple method : Characterization , parametric and isotherms study, Mater. Today Proc. **5** (2018) 3334-3345.
13. Giusto L. A. R., Pissetti F. L., Castro T. S., Magalhães F. - Preparation of Activated Carbon from Sugarcane Bagasse Soot and Methylene Blue Adsorption, Water Air Soil. Poll. **249** (2017) 1-10.
14. Ahmed M. J. - Adsorption of quinolone, tetracycline, and penicillin antibiotics from aqueous solution using activated carbons: Review, Environ. Toxicol. Pharmacol. **50** (2017) 1-10.
15. Genç N., Dogan E. C. - Adsorption kinetics of the antibiotic ciprofloxacin on bentonite, activated carbon, zeolite, and pumice, Desalin. Water Treat. **53** (2015) 785-793.
16. Bach L. G., Van T. T., Nguyen T. D., Van P. T., Do S. T. - Enhanced adsorption of methylene blue onto graphene oxide-doped XFe 2 O 4 (X = Co, Mn, Ni) nanocomposites: kinetic, isothermal, thermodynamic and recyclability studies, Res. Chem. Intermed. **44** (2018) 1661-1687.
17. Li J., Yu G., Pan L., Li C., You F., Xie S. - Study of ciprofloxacin removal by biochar obtained from used tea leaves, J. Environ. Sci. **73** (2018) 20–30.
18. Bajpai S. K., Bajpai M., Rai N. - Sorptive removal of ciprofoxacin hydrochloride from simulated wastewater using sawdust: Kinetic study and effect of pH, Water SA **38** (2012) 673–682.
19. Zhang C. L., Qiao G. L., Zhao F., Wang Y. - Thermodynamic and kinetic parameters of ciprofloxacin adsorption onto modified coal fly ash from aqueous solution, J. Mol. Liq. **163** (2011) 53-56.
20. Li Z., Hong H., Liao L., Ackley C. J., Schulz L. A., Macdonald R. A., Mihelich A. L., Emard S. M. - Colloids and Surfaces B: Biointerfaces A mechanistic study of ciprofloxacin removal by kaolinitem Colloids Surfaces B. **38** (2011) 339-344.
21. Sun Y., Li H., Li G., Gao B., Yue Q., Li X. - Characterization and ciprofloxacin adsorption properties of activated carbons prepared from biomass wastes by H_3PO_4 activation, Bioresour. Technol. **217** (2016) 239-244.